Fatigue Behavior of 3-D Triaxial Braided Composites

Carlos K. Gethers[1]
Robert L. Saddler[2]
V. Sarma Avva[3]

Introduction

Composite materials have been used for a myriad of applications ranging from common commodity goods to advanced structural applications in the marine, automotive, and aerospace industries [1]*. Typically, due to their high specific modulus and strength, laminated composites find greater uses in structural applications. But, as the aforementioned industries increase their usage of these composites, design limitations associated with these materials need to be addressed. By virtue of the inherent geometrical lay-ups of laminated composite structural components, non-uniform stresses in the various layers and directions may take place under loads. These stresses in turn induce interlaminar shear and normal stresses at the 'free' boundaries or edges [2] of composite laminates resulting in damage and or premature failures [3]. These undesirable characteristics have lead to the adaptation of existing textile industry processes to produce fibrous preforms with integrally braided and woven structures. Preforms are fabricated using fiber tows (yarns or bundles) in the textile processes such as braiding, knitting, weaving, etc. An example of the fibrous preform used in this study is shown in Fig. 1. Structural preforms are developed using textile technologies such as bi- and tri-axial weaving, weft inserted knitting, filament winding, non-woven, braiding, and 3-D weaving and braiding [1]. The composite structural components made with various preform fabricating technologies exhibit some advantages, selectively, over traditional 2-D laminated composites. Specifically, the salient advantages are : Improved through-the-thickness strength, near net shape components, and lower cost of manufacturing, if the process could be automated. However great the advantages are, textile composites will be too expensive if the preform processes are not automated. Machine down time (for example, the time spent in stringing the tows) must be reduced if this technology can have its full impact on industry. Presently, the process is found to be time consuming, laborious, difficult to control (in terms of maintaining a consistent braid angle) and harsh on the fibers. Despite these problems, the textile composite preform technologies are advancing at a rapid pace currently.

The objectives of this research are: to braid 3-D tubular preforms with a consistent architecture (radially and longitudinally); to achieve uniform panel thickness; to study the tensile and fatigue behavior of 3-D triaxial braided graphite/epoxy composite materials.

---

[1]Graduate Research Assistant, [2]Adjunct Associate Research Professor, and [3]Professor., Center for Composite Materials Research and Mars Mission Research Center, Department of Mechanical Engineering, North Carolina Agricultural and Technical State University, Greensboro, NC., USA

** The numbers in square brackets refer to the list of references appended to this paper.*

Materials and Specimen Configuration

For this study coupons were fabricated using BASF G30-500 12k fiber tows with Epon 828 matrix and Jeffamine T-403 as a catalyst. Earlier studies were conducted to establish the tensile properties of 3-D preforms braided to near net shape. Results from these studies indicate that many factors such as preform quality, compaction, braid angle, degree of curing, fiber volume ratio, and others affect the mechanical properties. Based on the preceding experience, a new tensile test coupon geometry was decided upon. Since braiding of tubular preforms typically takes place with tow angles at $\pm\beta$, they do not, in general, provide comparable strengths to laminated composite components (e.g., filament wound tubes, etc.). With this in the background, the axial direction of the tube is reinforced with 46% of axial tows. A flat panel was obtained by slicing a 1.5 inch (38.1 mm) -internal diameter- tubular 3-D braided preform through compression molding. The fiber placement architecture of this panel is now 3-D triaxial. This technique yields three specimens per panel and up to nine coupons per tube of about 35-36 inches (889-914 mm). Typical coupon geometry is shown in Fig. 2. The coupons are 10 inches (254 mm) long with a length in the dog-boned portion of about 5 inches (127 mm), and 1 inch (25.4 mm) in width. The thickness of each coupon is 0.1 ± 0.002 inches (2.54 ± 0.0508 mm). Coupons were dogboned so as to permit failures within the neck-down section. Even though straight sided coupons will provide the same results as waisted or dogbonned coupons, it has been shown [3] that at higher load amplitudes waisted or dogbonned coupons will reduce or eliminate tab failures (a typical phenomenon in straight-sided coupons).

Preform Fabrication and Compaction

All preforms were fabricated on a four-step circular braiding machine. The name "four-step" comes from the four distinct carrier movements made by the braider to complete one braiding cycle (see Fig. 3). The braiding machine consists of an elevated bobbin, table of rotating concentric column and carrier rings, pneumatic actuators that alternately power the columns and carriers, and elastic tension control devices (TCDs). This particular braiding machine has 180 braider (moving) carriers and 150 axial (fixed) carriers. Connected to these carriers are elastic bands (TCDs). These bands are used to vary the tension placed on the fiber tows during braiding.

The process of stringing consists of tying fiber tows to tension control devices (TCDs), hanging the fiber over hooks on the bobbin, and tying the free end of the fiber to another TCD. Both tied ends were taped to prevent unraveling. If the fibers unravel during braiding, the geometry of the braid may be altered - changing the braid angle, direction of the fibers, or even producing a hole in the preform (see Fig. 4). Braider yarns are strung with braider yarns and axial yarns with axial yarns. This is critical because of the tension and height differences that must be maintained between the two (sets of yarn). Braider yarns were strung with little or no tension. This was done to permit free movement of the yarns throughout the preform during fabrication. Because the braider yarns are interlacing throughout the preform, they have to be strung four to five inches below the axial yarns.

The axial yarns have tension on them so as to permit them to remain straight during the braiding process. The length of the axial yarns also dictates the final

length of the preform produced. The tension on the braider and axial yarns were controlled by the operator. If the tension was not maintained, this would result in a poor quality preform. If the axial fibers were strung too loosely, they would not be straight, as is desired in a preform. This problem is not as serious with the braider yarns because it permits them to be mobile during braiding. However, stringing the braider yarns too loosely could make braiding more difficult and increase the likelihood of fiber looping (see Fig. 5). If the axial fibers were strung with "too much tension", the tied fiber ends would tend to unravel and the height of the bobbin supporting the fibers decreases

A mandrel was hung from the elevated bobbin and the fibers were clamped at the top of the mandrel. The fibers were lubricated with a light spray of water to prevent breakage and then the braiding process was started. Pneumatic actuators were fired in a sequence necessary to complete one braiding cycle. After every two braiding cycles, it was necessary to compact the fibers to the desired braid angle ("beating up the fibers"). During this process some fiber breakage was noticed. However, it is believed that this fiber breakage does not have a significant effect on the resulting mechanical properties. When the desired braid length was reached, the bottom of the preform was clamped and removed from the braiding machine.

Panel Consolidation and Processing

The preform was slit axially using the axial fibers as guides. This was done so that no axial fibers would be cut. The preform was then rolled out into a rectangular shape, and baked in an oven for 1 hour at 212°F (100°C) to remove water applied during braiding. The preform was then cut into three 11.5 x 5 inch^2 (292 x 127 mm^2) rectangles and the braid angle of each panel was measured. Fig. 6 shows the geometry and dimensions of the preform before and after it was slit. This figure also shows the positions of specimens relative to their location in the preform.

After preparing the preform, a steel compression mold was waxed and buffed to aid in the release of the cured panel. Components of the mold assembly should be disassembled or reassembled, as the case may be, in the same manner in which it was machined. Permanent markers to identify the alignment of mold components is critical and essential. This was suggested to permit the proper mold assembly after each use.

The mold was designed so that the desired panel thickness is controlled by placing positive metal stops along the side edges (see Fig. 7). The desired panel thickness (and thickness of the metal stops) was 0.100±0.002 in. (25.4±0.0508 mm). But, due to tolerance variations along the side edges of the mold, it was necessary to augment the thicknesses of the metal stops. This was done by adding strips of 0.004 in. (0.1016 mm) nylon tape to the edges of the mold where the stops were placed. This procedure produced panels with a thickness variation of ±0.002 in. (0.0508 mm).

Resin preparation consisted of measuring, heating, and mixing approximately 11 ounces (300 grams) of Epon 828 resin with approximately 4.5 ounces (126 grams) of Jeffamine T-403 catalyst. The mixture was then evacuated in an evacuation chamber for approximately 10 minutes at 1 torr (1 mm Hg or 0.019

psi). The resin was then removed from the chamber and a 0.25 in. (6.35 mm) layer was poured into the bottom of the mold. The preform was inserted into the mold at an angle to prevent the entrapment of air between the resin and the preform. The remaining resin was then poured atop the preform. The preform was pressed down using metal bars to prevent floating during matrix/preform evacuation. The matrix and preform were evacuated at 1 torr (mm Hg) for 20 minutes. The metal bars were removed and the metal stops were placed on the side edges of the mold. The plunger was then placed atop the preform at an angle. This was also done to prevent any trapping of air in the matrix. The plunger was allowed to settle and excess resin was allowed to escape from the mold. Once the plunger was settled, the assembly was wrapped into a nylon bagging material and placed into a preheated press for curing. The panel was cured at 212 °F (100 °C) for 3 hours. Once the curing process was complete, the mold was allowed to cool to room temperature and then the composite panel was removed from the mold. The entire process takes about 4 hours.

Preparing Specimen and Testing

After removal of the panel from the mold, the ends and the edges of the panel were trimmed and sanded. The thickness was measured using a granite surface plate and a dial gage. Twenty two measurements were taken through the length and width of the panel, and the thickness variation for each panel was assessed. From these measurements, the average panel thickness was found to be 0.100 ±0.002 in. The panel was then properly marked for machining. An axial line was scribed parallel to an axial fiber and two more lines are scribed orthogonal to this line indicating the desired 10 inch (25.4 mm) length (per ASTM standard D 3039). It is necessary that the coupons are machined so that the axial fibers are parallel to the loading direction. For this reason great care was taken to make sure that all lines were accurately drawn and straight. The designation for the location of each coupon in the panel was also engraved. Three dogboned specimens were obtained from each panel. Specimens were tabbed with cross ply fiber glass/ epoxy material. Tabs were secured to the specimen with FM 300 Interleaf high strain modified resin film. The cure cycle for the film was 212°F (100 °C) at 1000 psi (689 kN/m^2) for 3 hours. Once the coupons were tabbed, they were ready for testing.

Tensile and fatigue tests were performed using dogbonned 3-D triaxial braided $[0_{12k}/\pm30_{12k}]_{46\%\ axials}$ graphite/epoxy composite specimens. The tensile tests were performed on a 50,000 lbf (23,000 kg) load frame under stroke control with a loading rate of 0.02 in/min (0.508 mm/min). Strain gages were mounted on one surface of the specimen to obtain the stress strain curve as well as the ultimate failure strength. A total of nine specimens were tested primarily to establish the static strength at failure.

Tension-tension fatigue tests were performed to determine the stress vs. number of cycles to failure (S-N) behavior and residual tensile strength of the textile composites. Testing was performed on a 50,000 lbf (23,000 kg) load frame fitted with hydraulic grips. All testing was conducted at room temperature and at a frequency of 10 Hz. The load amplitude, R, (ratio of minimum to maximum load) was set at 0.1 and all coupons were tested to failure or run out at one million cycles. Coupons that survived one million cycles were statically tested to

determine their residual strength. A total of 45 specimens were tested in this mode.

Temperature rise during the fatigue tests was monitored on some specimens. A non-contacting temperature gun was used to measure the increase in temperature of specimens (at mid-section) tested at 60%, 70%, and 80% of the average ultimate tensile strength. This particular data was recorded manually.

Results and Analysis

Nine axial tension tests were performed in order to determine the average ultimate tensile strength and the modulus of elasticity. Fiber volume percents were also evaluated. The average strength at failure, modulus of elasticity and the fiber volume ratio are found to be 116 ksi (800 kN/m^2), 10.88 Msi (75 GN/m^2), and 49.5%, respectively (see Table 1). Fig. 8. shows a typical stress-strain response of the material tested. The average tensile strength of the composites was then used to set the percentage of stress (load) ratios in the tension-tension fatigue tests that followed.

Approximately 45 coupons were tested in fatigue mode(see Fig. 9). The random test matrix that was used is shown in Table 2. Tests were conducted at 50%, 60%, 70%, and 80% of the composite's ultimate tensile strength. The 50% data represents four run out points and one failure in the fifth decade. This last failure could be due to poor consolidation, , or machining errors. Very little scatter appears in the 60% data and the points are well grouped. There is also one run out at this amplitude level. The results at higher amplitude levels show more scatter (three decades) than at the lower amplitudes (one to two decades). This may be possibly due to the fact that at higher load levels, any minute flaws present in the material from consolidation, machining, etc., operations may get amplified rapidly and irregularly leading to premature failures. Similar scatter was reported by Whitney [4] who performed tension-tension fatigue tests with T300/934 laminates at 10 Hz.

The number of coupons available for residual tensile strength tests depended upon the results of the tension-tension fatigue tests. Out of 45 coupons, five survived one million fatigue cycles and were tested for their residual tensile strength (see Fig. 10). All but one of the specimens were from the 50% regime (P5 B-R tested at 60%). There was a 1.0% to 28.0% decrease in the residual tensile strength after fatigue. It was noticed that the residual strength may be proportional to the visible matrix damage. Coupon P8 T-R (11,468 lb or 5201 kg), tested at 50%, had virtually no or very little visual damage where as coupon P5 B-M (8,343 lb or 3783 kg), tested at 60%, had much more in comparison (see Fig. 11). There is little change in the residual strengths of coupons P5 B-M (8,613 lb or 3900 kg)and P5 B-R (8,343 lb or 3783 kg). This is not the case, however, with coupons P8 T-R and P8 M-L.

During fatigue testing at 60%, 70%, and 80% of the load amplitude, the temperature rise was monitored (see Figs. 12a-c). The temperature response of coupons at 70% (see Fig. 12b) of load amplitude (P6 B-R) is similar to that of unidirectional graphite/epoxy (T300/5208) composites reported in [5]. The temperature increases as if it is heading to an almost constant value, and then rapidly and linearly increases until just before failure. At 80% of the load amplitude, the temperature response is somewhat linear. This is due to the short

fatigue life of the specimen as is evident in Fig. 12c. Even so, close observation of both figures will show the similarities between the curves. The recording of temperature at 60% (Fig. 12a) was aborted at 8,000 cycles due to other reasons. However, this response is again similar to that shown in Fig. 12b. A sudden increase in temperature was observed before failure takes place and this increase was found to vary from specimen to specimen.

All tensile fracture surfaces show little fiber pull out and matrix damage (almost clean fracture surface). Failure initiation at each load level appears to begin at the coupon's "free" edge between the cut braider tows. After initiation, cracks appear to propagate in a direction parallel to the braider tows towards the center of the coupon. Each load level produced distinguishable failure surfaces. Coupons fatigued at 50% have little matrix damage and resembled tensile failures (see Fig. 13). Where as, coupons tested at 60% of the average tensile strength suffered severe matrix damage (see Fig. 14). Characteristics of this load level are severe fiber debonding and axial fiber pull out. This type of brush-like fracture is similar to that of fiber reinforced laminated composites reported in [6]. 70% load levels produced failure surfaces with less matrix damage than those tested at 60% (see Fig. 15). The path of crack propagation can be more easily seen in these coupons than in others. This path shows fiber debonding and pullout as was seen in coupons tested at 60%. Failures at the 80% load amplitude resemble tensile failures and have little matrix damage (see Fig. 16). However, different failure modes, as observed here with limited data base, did not necessarily correspond to a difference in the failure lives.

Conclusions

3-D triaxial braided $[0_{12K}/\pm 30_{12K}]_{46\%\ axials}$ graphite/epoxy composites were successfully fabricated using compression molding techniques, and tested to determine their average ultimate tensile strength and the tension-tension fatigue behavior, including residual strength. Preform architecture was consistent, even though the braid angle was difficult to maintain. Fiber loss was noticed during the braiding process. However, it is believed that this fiber loss did not have a significant effect on the resulting mechanical properties. The consolidation procedure was sufficient to produce good quality composite panels. The average failure strength, modulus, and percent fiber volume were found to be 116 ksi (800 MN/m^2),10.88 Msi (75 GN/m^2), and 49.5%, respectively.

References

[1] Li, Wei and El Sheik, A., "The Effect of Processing Parameters on 3-D Braided Preforms for Composites," Mars Mission Research Center, College of Textiles, North Carolina State University, Raleigh, NC.

[2] Klein, J.A., Senior Editor., "Braids and Knits: Reinforcement in Multidirections", *Advanced Composites,* September / October, 1987.

[3] Avva, V. S., Saddler, R. L., Raju, I. S., "Emerging Use of Textile Preform Technologies in Aerospace Structural Composites," Center for Composite

Materials Research, Department of Mechanical Engineering, North Carolina A & T State University, Greensboro, NC.

[4] Whitney, J. M., "Fatigue Characterization of Composite Materials," Fatigue of Fibrous Composite Materials, ASTM STP 723, American Society for Testing And Materials, 1981, pp. 133-151.

[5] Awerbuch, J. and Hahn, H. T., "Fatigue and Proof-Testing of Unidirectional Graphite/Epoxy composite," *Fatigue of Filamentary Composite Materials,* ASTM STP 636, K. L. Reifsnider and K. N. Lauraitis, Eds., American Society for Testing and Materials, 1977, pp. 248-266

[6] Curtis, D. C., Moore, D. R., Slater, B. and Zahlan, N., "Fatigue Testing of Multi-Angle Laminates of CF/PEEK," Journal of Composite Materials, Vol. 19, November 1988, pp. 446-452.

[7] Li, W., Hammad, M., El-Sheikh, A.,"Mechanics of Three-Dimensional Braiding, Basic Requirements for Process Automation," Mars Mission Research Center, College of Textiles, North Carolina State University, Raleigh, NC.

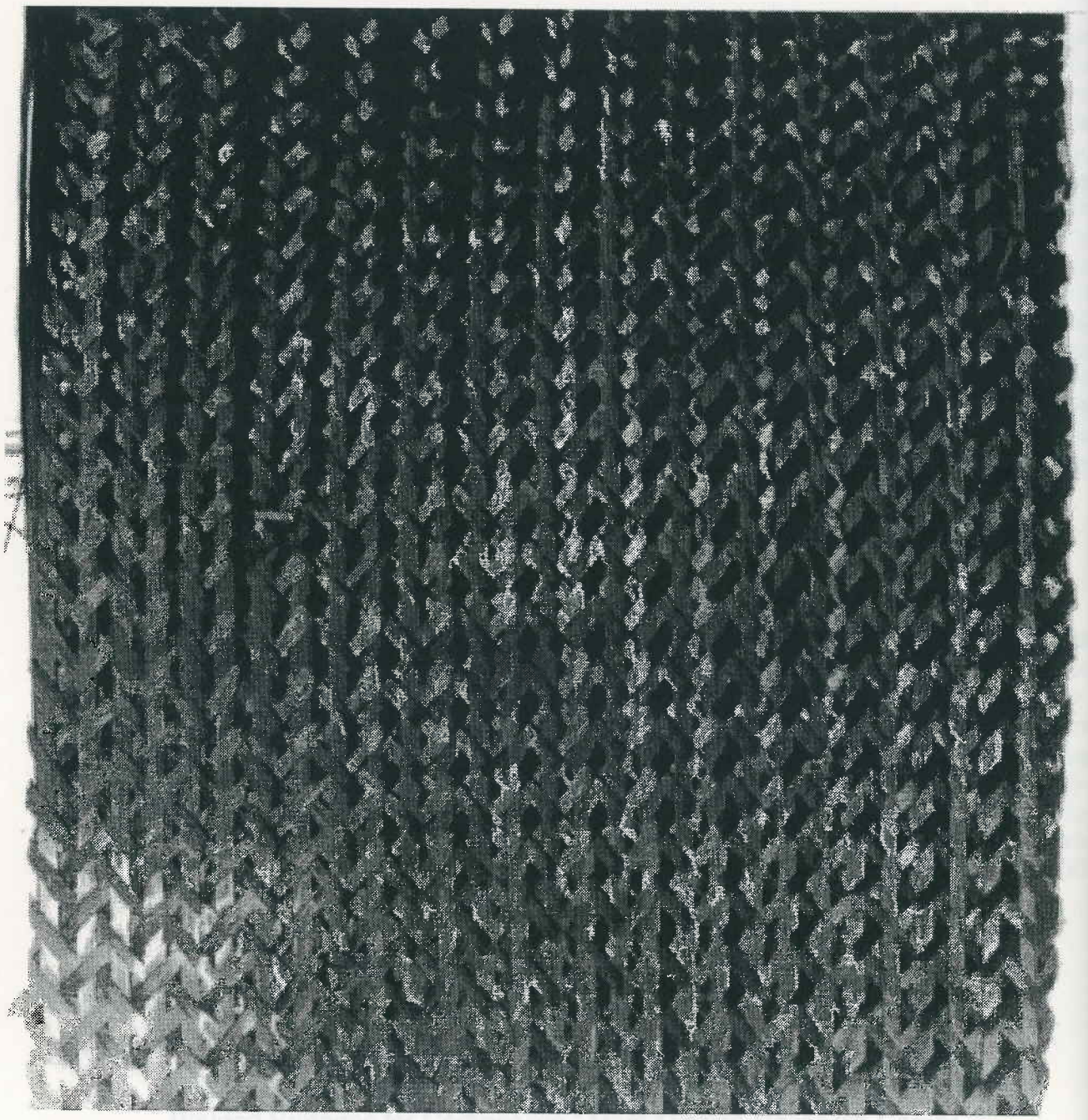

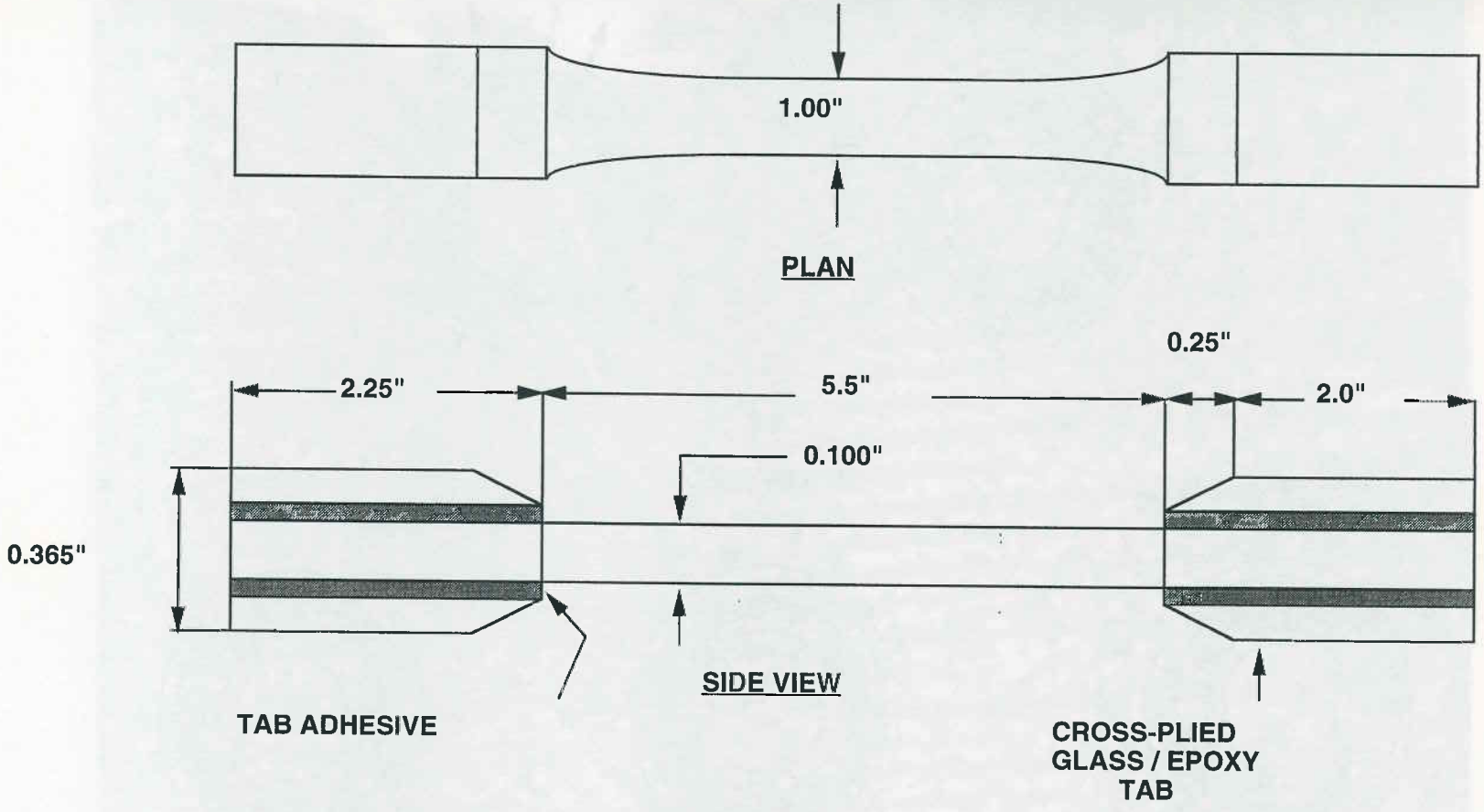

Figure 2. Test specimen configuration

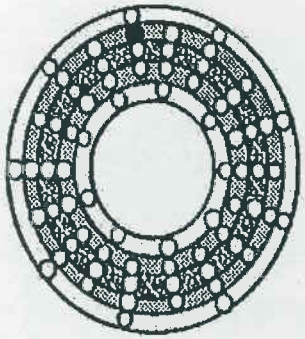

The original position

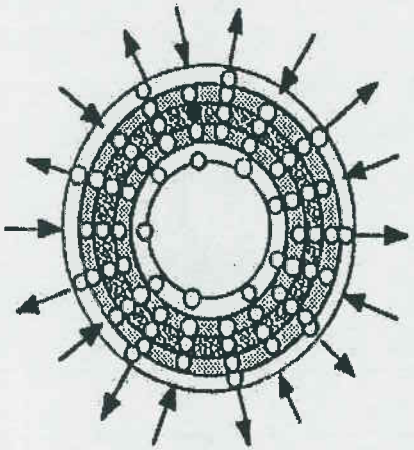

The first step

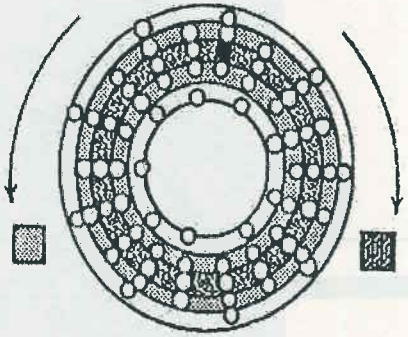

The second step

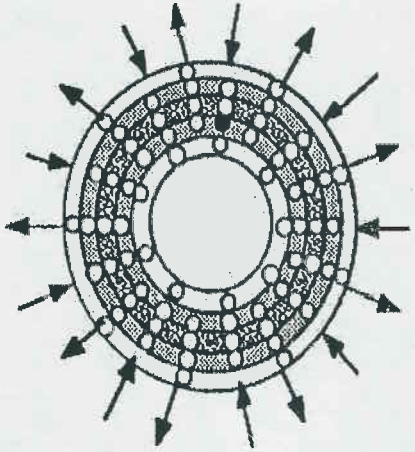

The third step

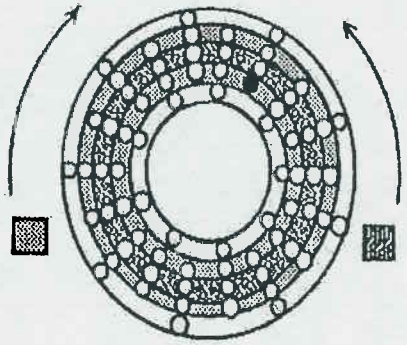

The fourth step

The third step

The fourth step

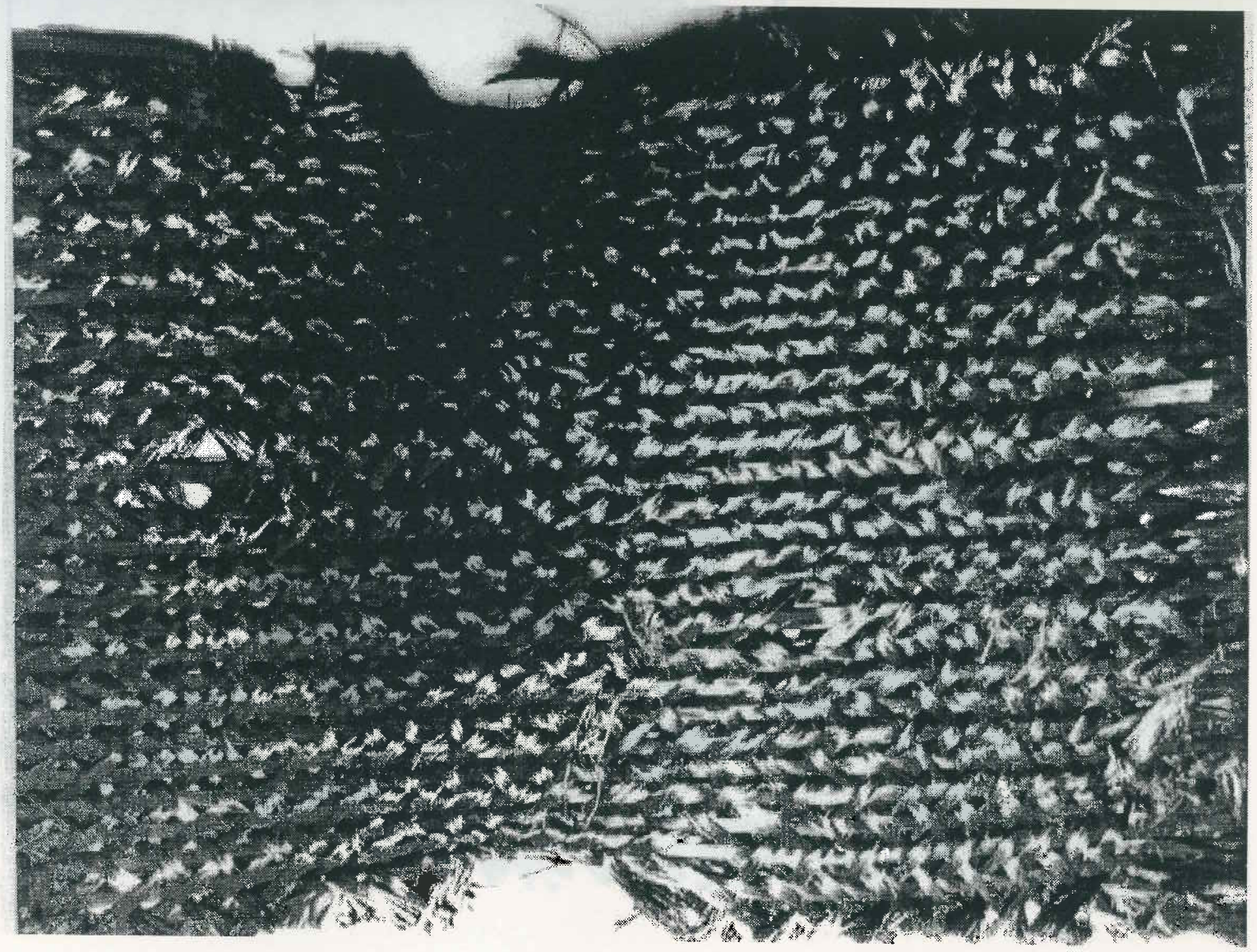

Figure 4. 3-D preform braided with holes.

3-D BRAIDED CYLINDER

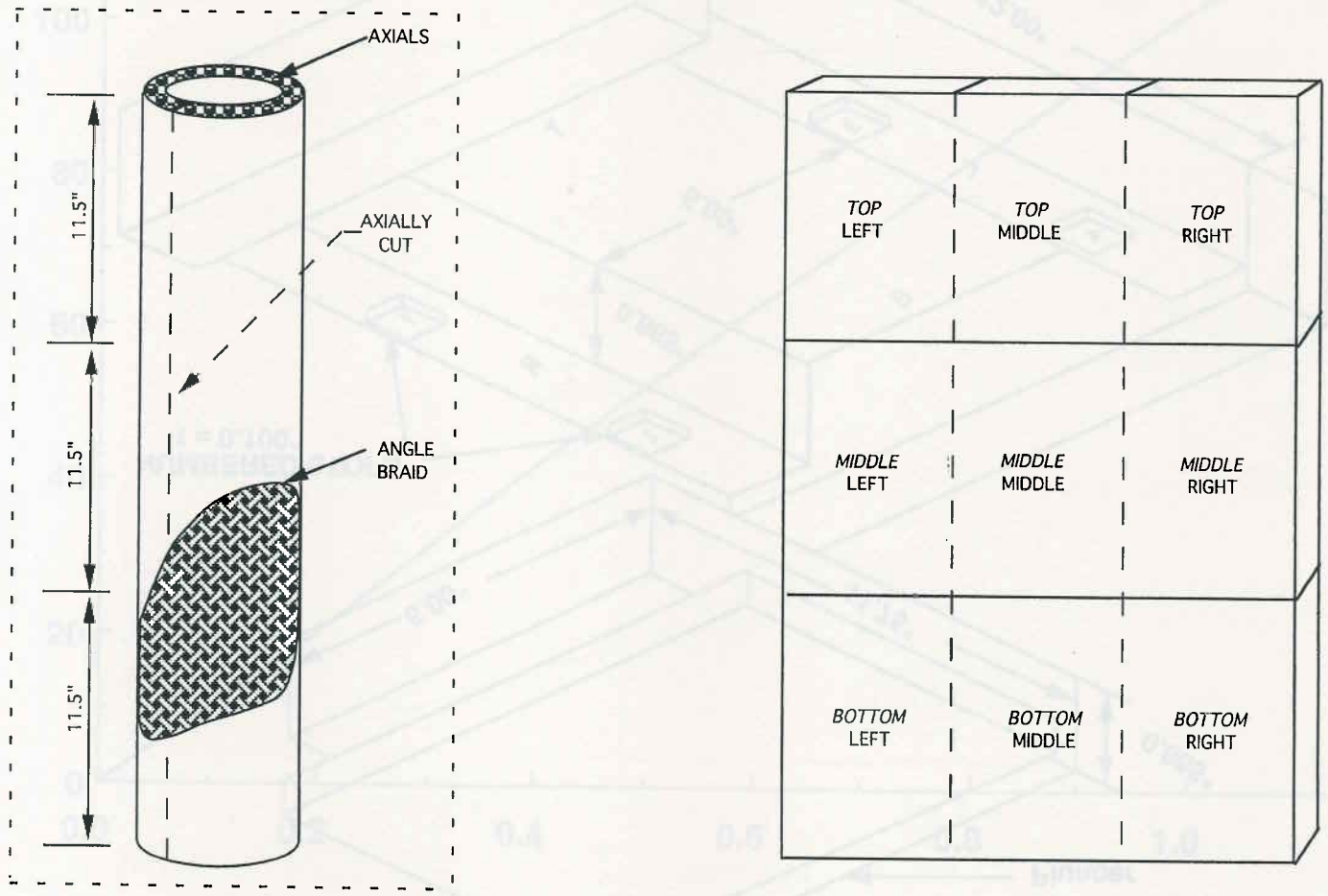

Figure 6. Preform dimensions and coupon locations with respect to tube/panel.

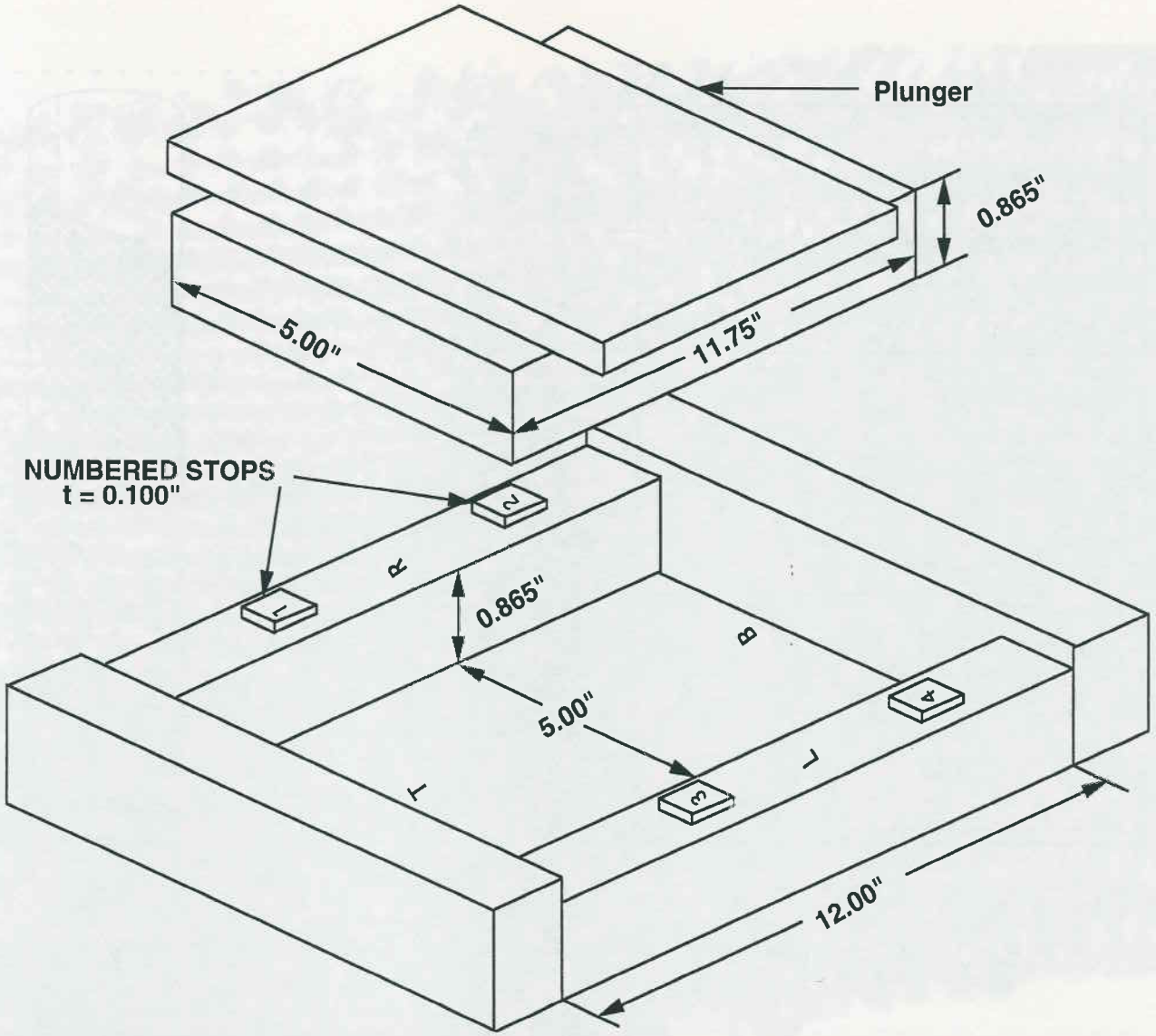
Plunger
0.865"
5.00"
11.75"
NUMBERED STOPS
t = 0.100"
2
1
R
0.865"
B
5.00"
4
3
L
J
12.00"

120

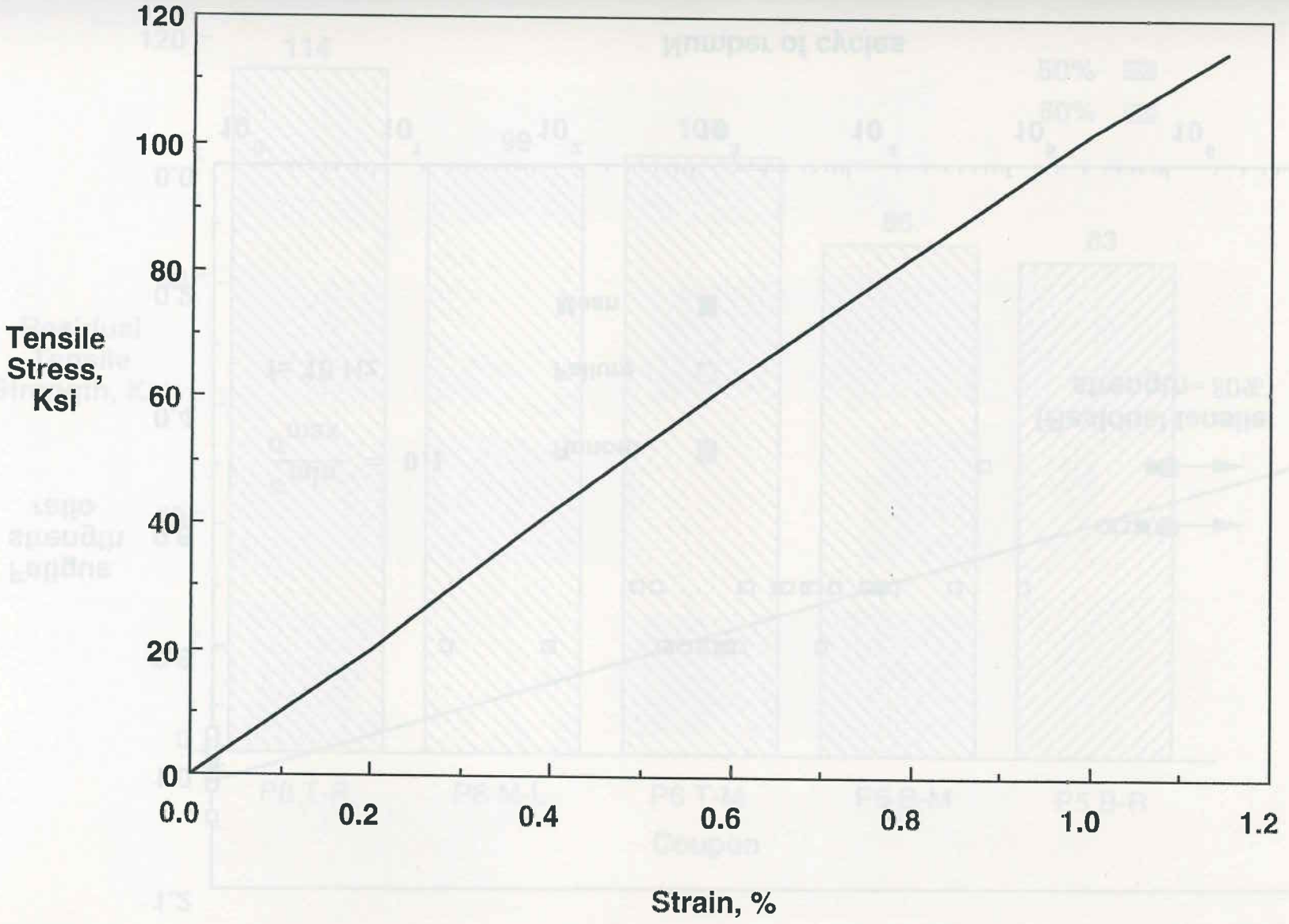

Figure 8. Typical stress-strain response.

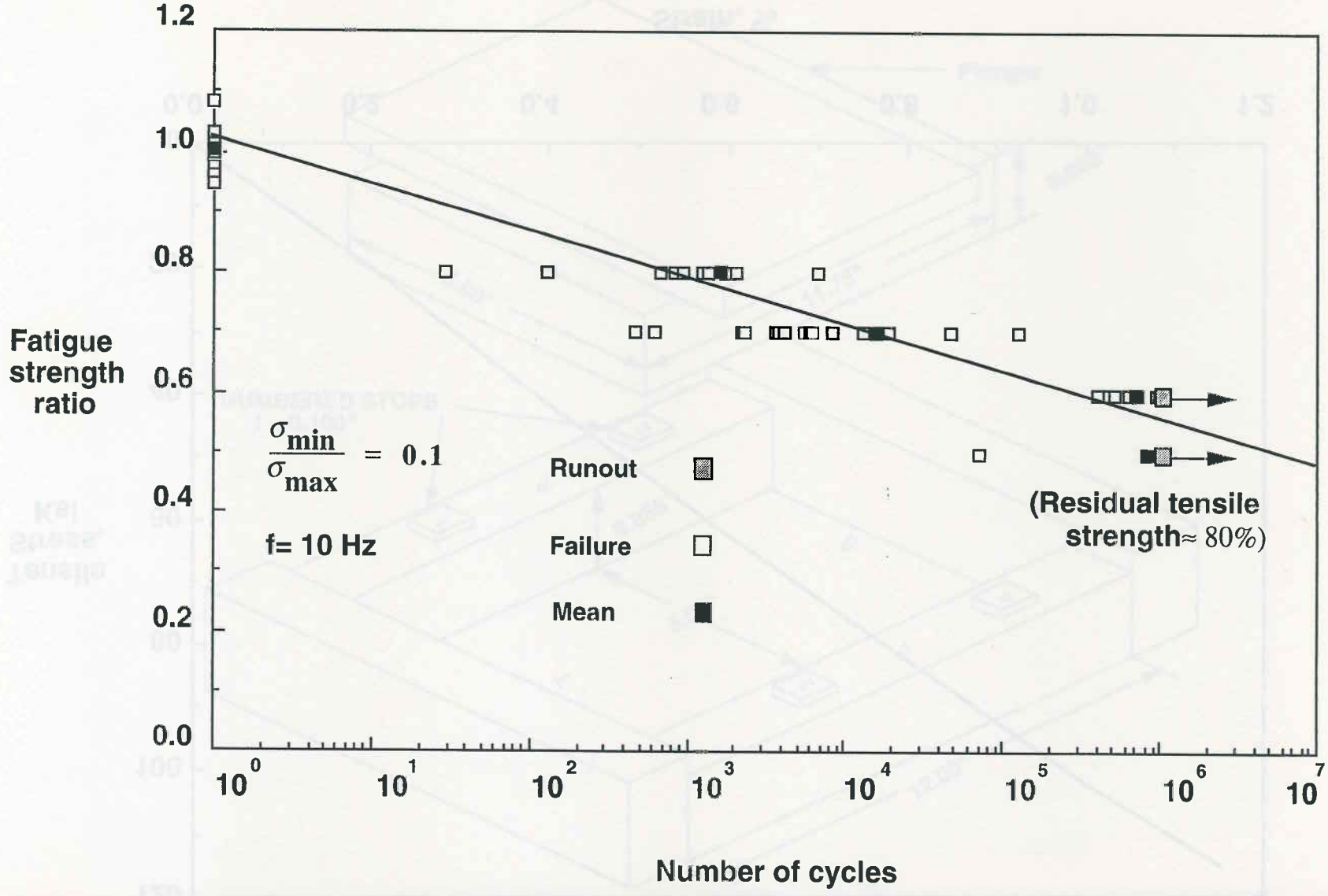
1.2
1.0
0.8
0.6
0.4
0.2
0.0
Fatigue strength ratio
$\frac{\sigma_{min}}{\sigma_{max}} = 0.1$
f= 10 Hz
Runout
Failure
Mean
(Residual tensile strength≈ 80%)
10^0
10^1
10^2
10^3
10^4
10^5
10^6
10^7
Number of cycles


120
114
50%

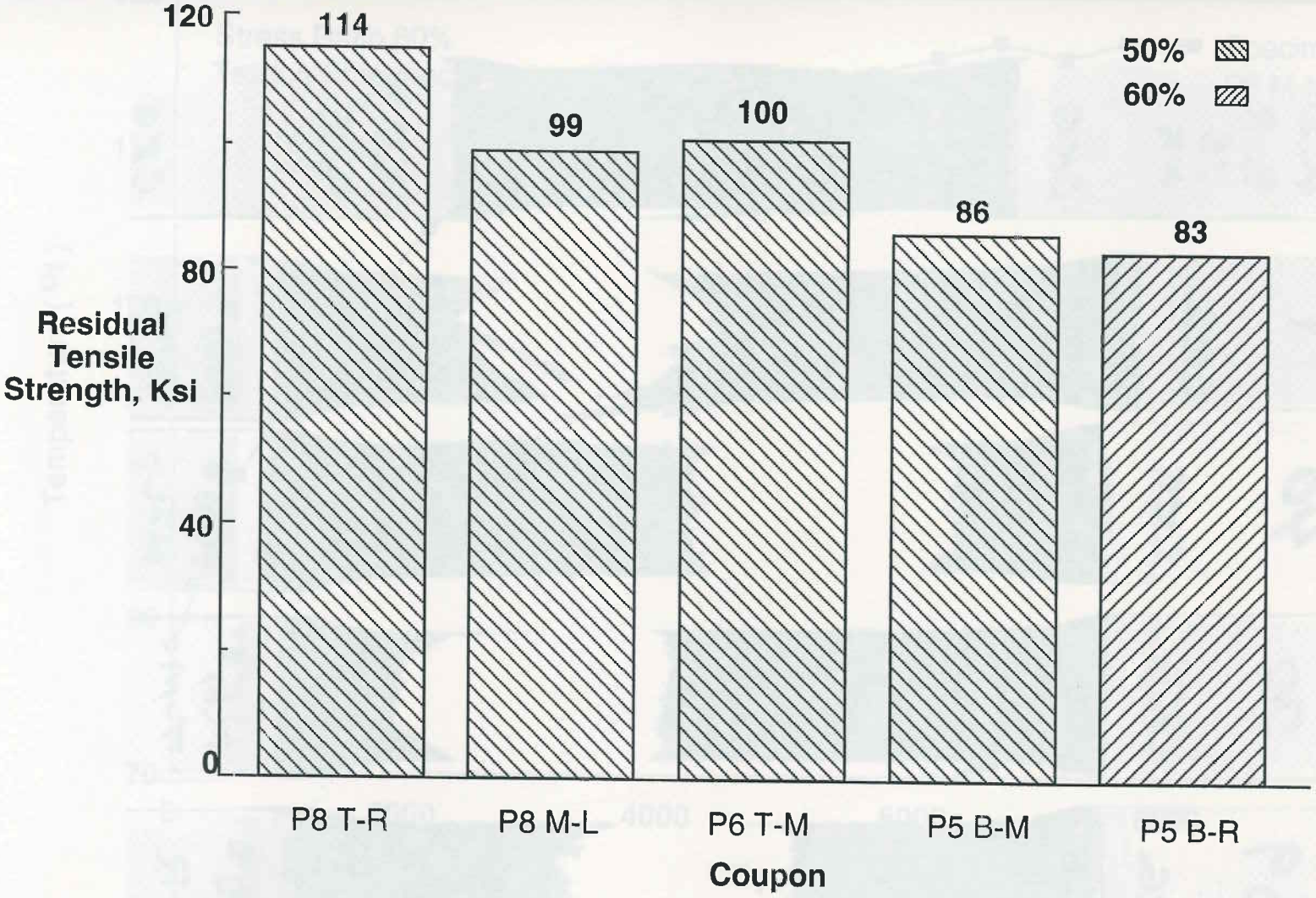

Figure 10. Residual tensile strength of coupons fatigued 1 million cycles.

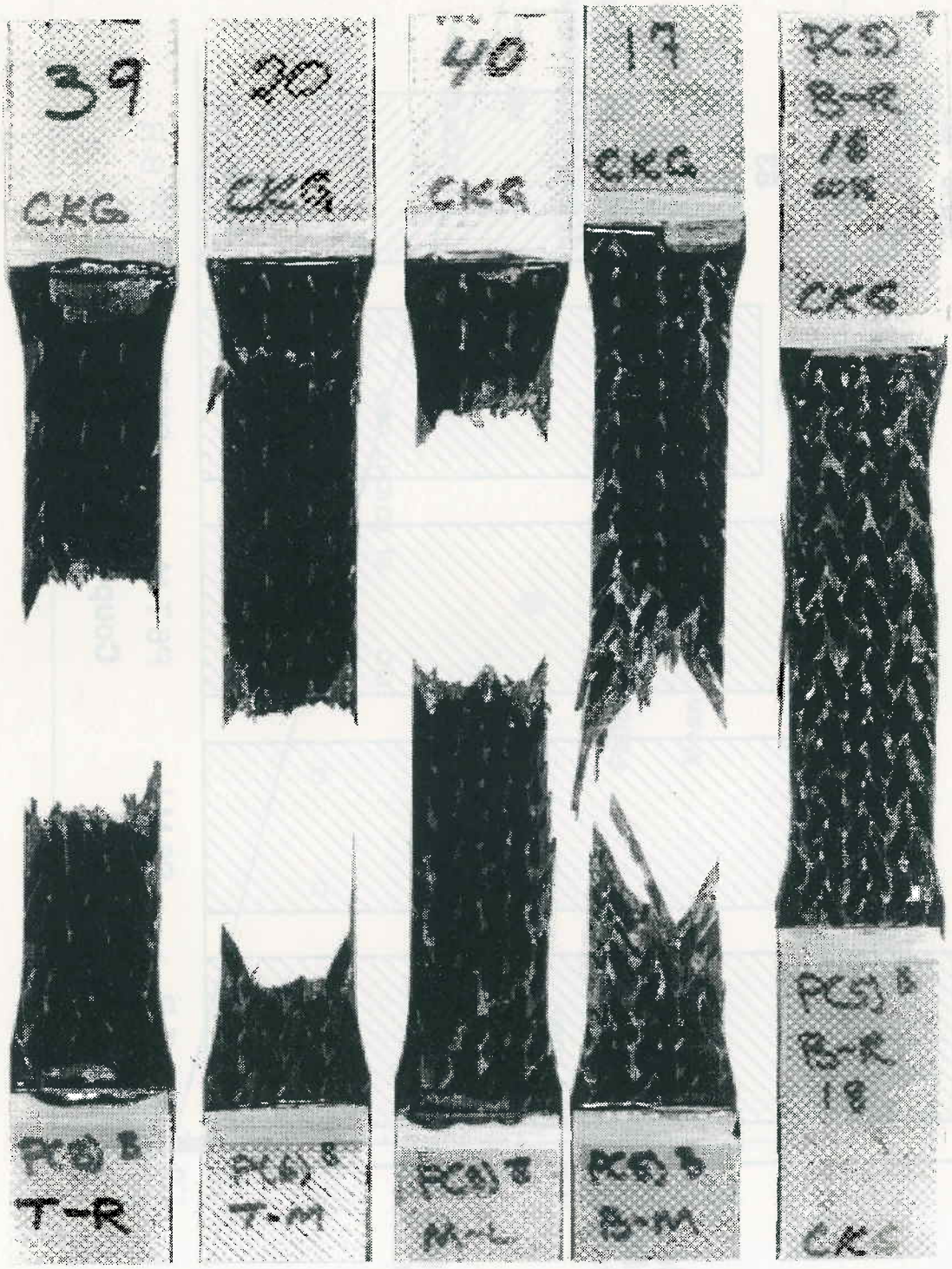

Stress Ratio 60%

Specimen

120

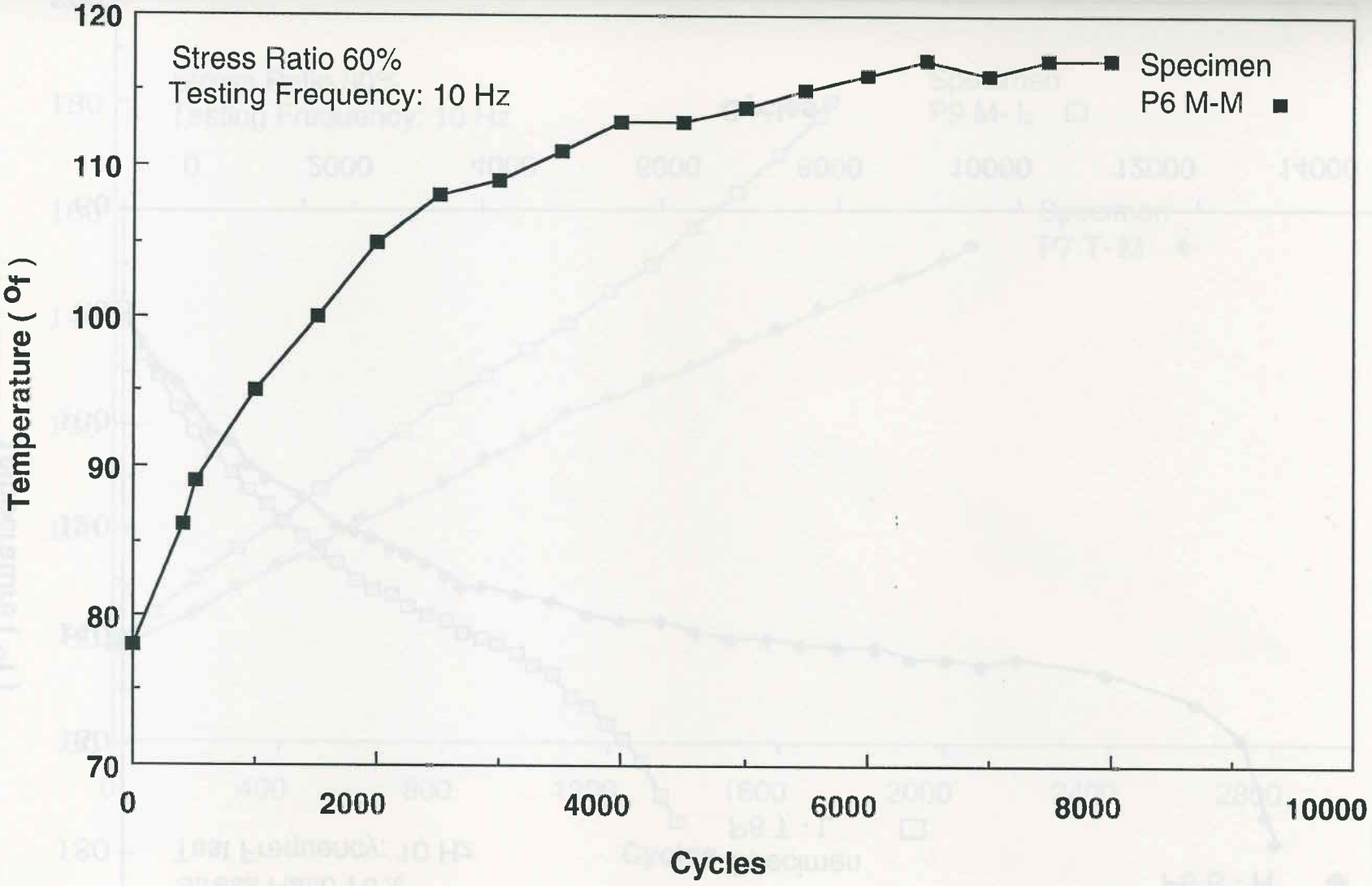

Figure 12a. Partial coupon temperature rise during fatigue at 60% UTS

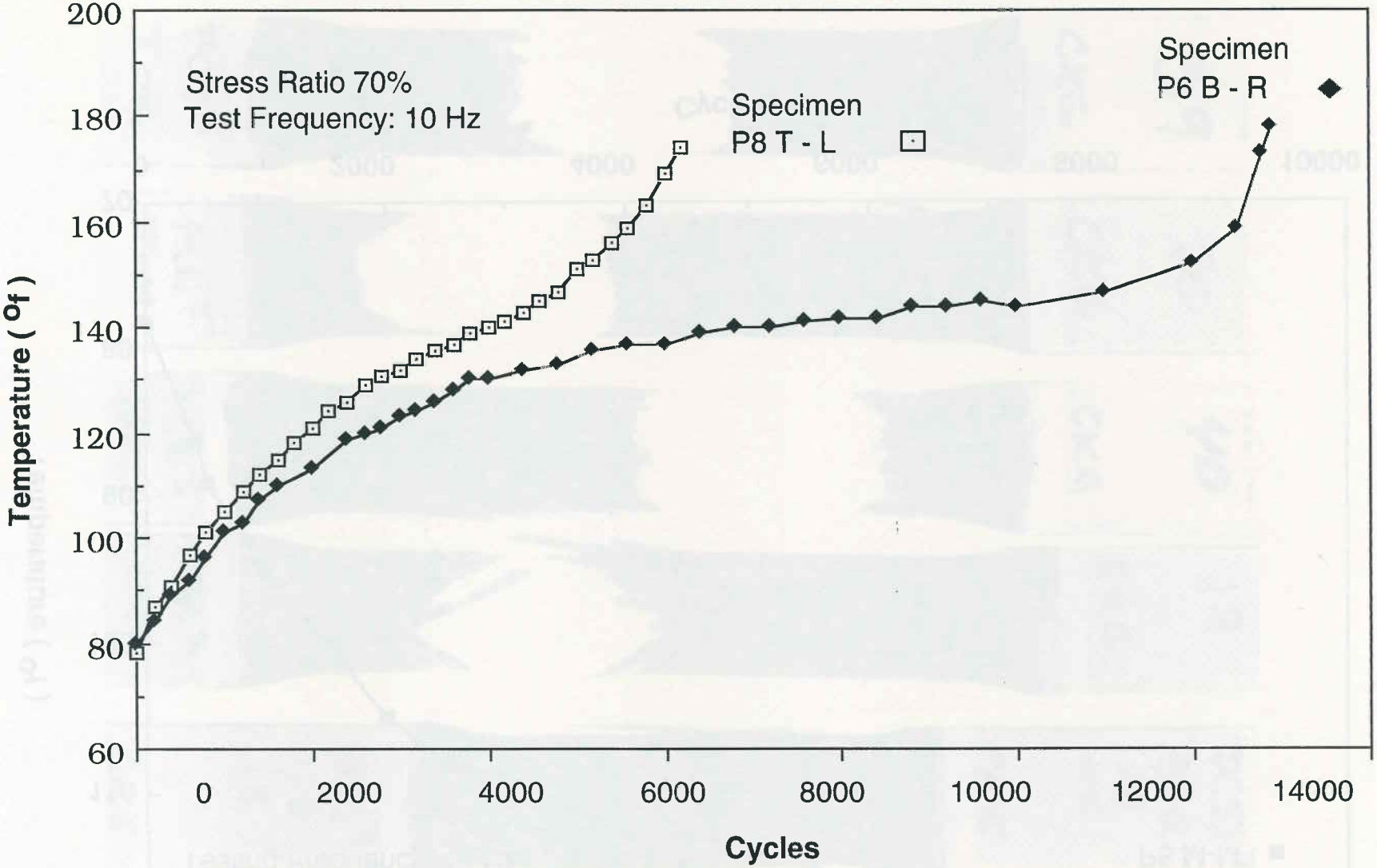

Figure 12b. Coupon temperature rise during fatigue at 70%

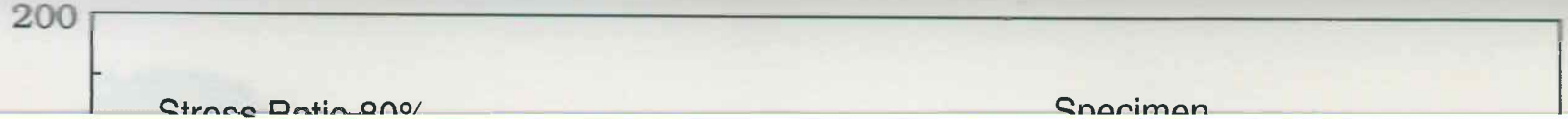

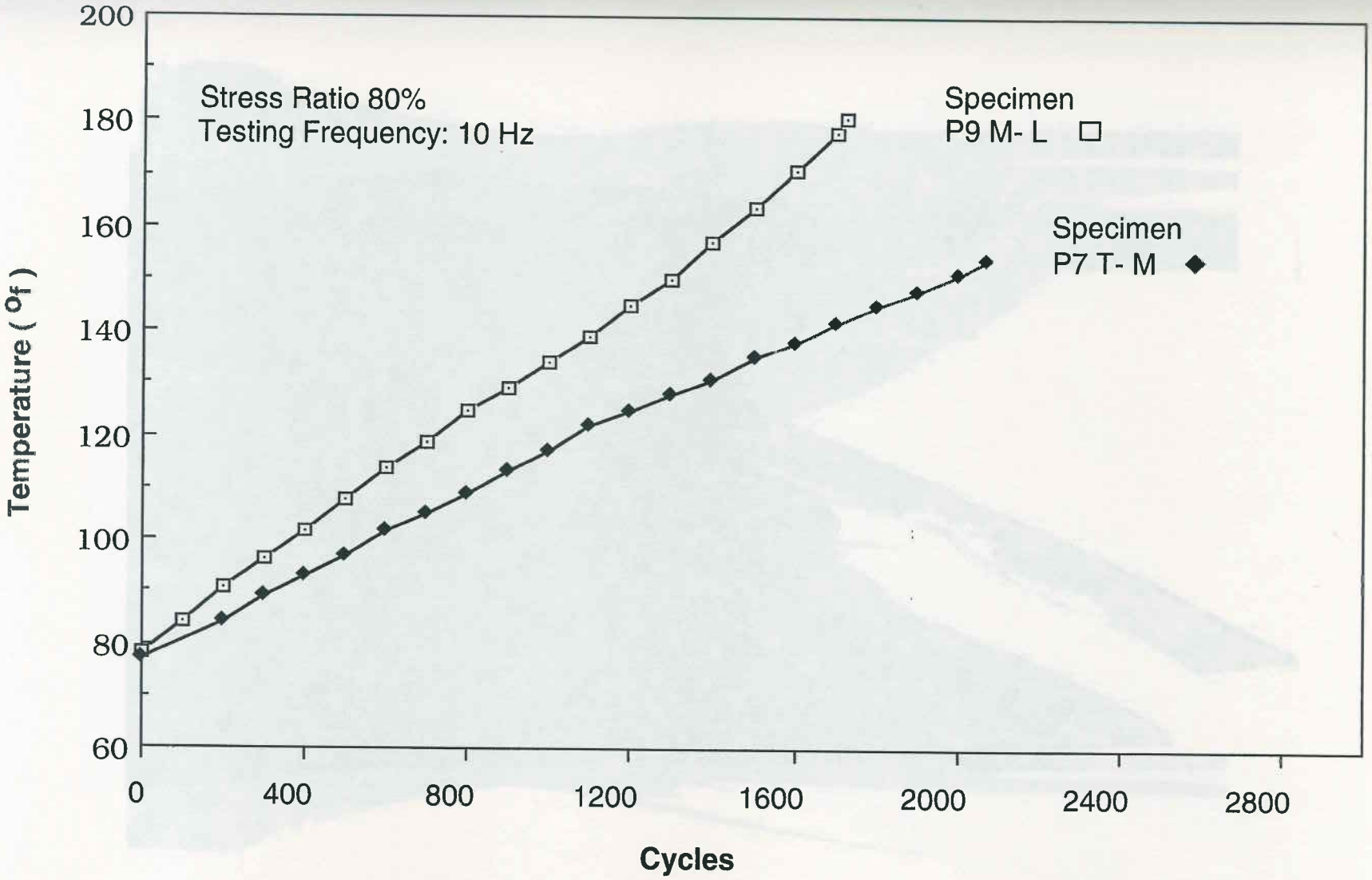

Figure 12c. Coupon temperature rise during fatigue at 80% UTS.

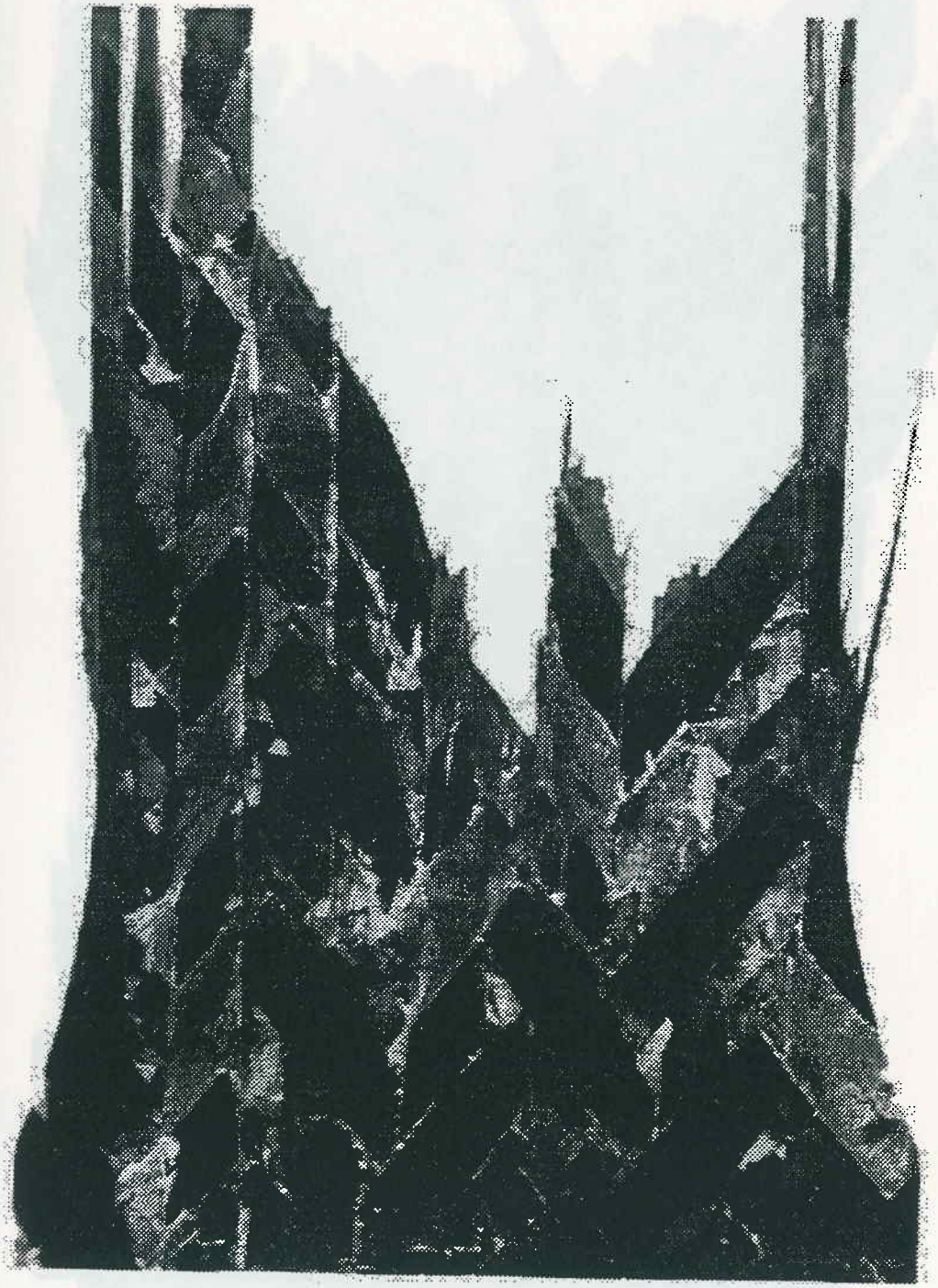

Figure 14. Typical failure surface of coupons tested at 60%.

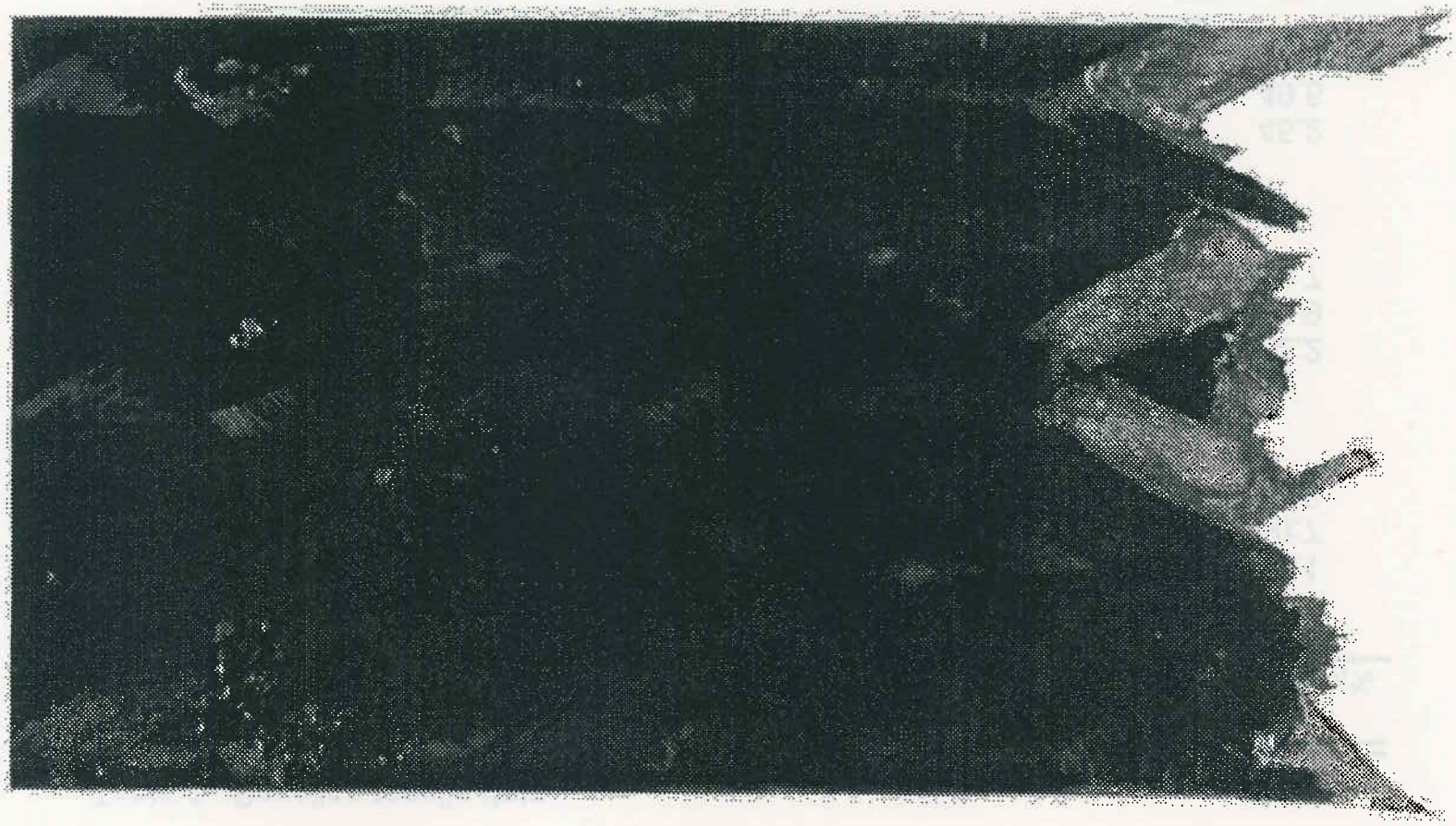

Figure 16. Typical failure surface of coupons tested at 80%.

Table 1. Baseline tensile data.

Material Designation	Ultimate Stress, ksi	Modulus Msi	Fiber Volume,%
Top Panel			
Left	112	10.38	49.1
Middle	117	11.31	50.7
Right	110	10.08	47.8
Middle Panel			
Left	117	10.15	52.2
Middle	115	10.19	50.9
Right	113	10.06	46.7
Bottom Panel			
Left	120	12.16	45.2
Middle	118	12.04	49.5
Right	126	11.58	53.3
Average	**116**	**10.88**	**49.5**

Table 2.-Random test matrix.

Average	**116**	**10.88**	**49.5**

Table 2.-Random test matrix.

Applied Load Amplitude			
50%	**60%**	**70%**	**80%**
P8 T-R	P8 M-R	P7 T-L	P8 M-M*
P8 M-L	P4 T-M	P5 T-M	P4 T-L
P6 T-M	P4 T-R	P8 B-L	P7 M-M
P5 B-M	P7 B-R	P5 T-L	P5 B-L
P4 M-M	P6 M-M	P8 T-M	P8 B-R
	P6 B-L	P7 M-R	P7 M-L*
	P5 B-R	P7 T-R	P7 B-M
	P8 T-L	P4 M-R	P6 B-M
	P6 B-R	P9 M-R	P7 T-M
	P8 B-M	P4 B-L	P4 B-R
	P7 B-L	P6 T-L	
	P6 M-R	P9 M-L	
	P4 B-M	P9 M-M	
	P6 M-L		
	P6 T-R		
	P8 T-L		
	P6 B-R		

* Not included in the data.